Progression of White Matter Hyperintensities Preceded by Heterogeneous Decline of Microstructural Integrity

Esther M.C. van Leijsen, MSc; Mayra I. Bergkamp, MSc; Ingeborg W.M. van Uden, MD, PhD; Mohsen Ghafoorian, PhD; Helena M. van der Holst, MD, PhD; David G. Norris, PhD; Bram Platel, PhD; Anil M. Tuladhar, MD, PhD; Frank-Erik de Leeuw, MD, PhD

Background and Purpose—White matter hyperintensities (WMH) are frequently seen on neuroimaging of elderly and are associated with cognitive decline and the development of dementia. Yet, the temporal dynamics of conversion of normal-appearing white matter (NAWM) into WMH remains unknown. We examined whether and when progression of WMH was preceded by changes in fluid-attenuated inversion recovery and diffusion tensor imaging values, thereby taking into account differences between participants with mild versus severe baseline WMH.

Methods—From 266 participants of the RUN DMC study (Radboud University Nijmegen Diffusion Tensor and Magnetic Resonance Imaging Cohort), we semiautomatically segmented WMH at 3 time points for 9 years. Images were registered to standard space through a subject template. We analyzed differences in baseline fluid-attenuated inversion recovery, fractional anisotropy, and mean diffusivity (MD) values and changes in MD values over time between 4 regions: (1) remaining NAWM, (2) NAWM converting into WMH in the second follow-up period, (3) NAWM converting into WMH in the first follow-up period, and (4) WMH.

Results—NAWM converting into WMH in the first or second time interval showed higher fluid-attenuated inversion recovery and MD values than remaining NAWM. MD values in NAWM converting into WMH in the first time interval were similar to MD values in WMH. When stratified by baseline WMH severity, participants with severe WMH had higher fluid-attenuated inversion recovery and MD and lower fractional anisotropy values than participants with mild WMH, in all areas including the NAWM. MD values in WMH and in NAWM that converted into WMH continuously increased over time.

Conclusions—Impaired microstructural integrity preceded conversion into WMH and continuously declined over time, suggesting a continuous disease process of white matter integrity loss that can be detected using diffusion tensor imaging even years before WMH become visible on conventional neuroimaging. Differences in microstructural integrity between participants with mild versus severe WMH suggest heterogeneity of both NAWM and WMH, which might explain the clinical variability observed in patients with similar small vessel disease severity. **(*Stroke*. 2018;49:1386-1393. DOI: 10.1161/STROKEAHA.118.020980.)**

Key Words: aged ■ cerebral small vessel diseases ■ humans ■ neuroimaging ■ white matter

White matter hyperintensities (WMH) are part of the spectrum of cerebral small vessel disease (SVD) markers and are frequently observed on magnetic resonance imaging (MRI) scans in individuals >60 years of age.[1–3] WMH are associated with cognitive decline and the development of dementia.[4,5] The pathophysiology of WMH remains poorly understood, in part, because studies on WMH and its progression have mainly used conventional MRI, thereby unable to assess its earlier stages that perhaps were not yet visible. Imaging techniques, such as diffusion tensor imaging (DTI), can possibly provide additional information on these earlier stages by the assessment of the microstructural organization of the white matter (WM).[6–9] Previous longitudinal studies have shown changes in baseline DTI parameters, that is, decreased fractional anisotropy (FA) and increased mean diffusivity (MD), that predicted incident WMH at follow-up.[10,11]

However, the temporal course of DTI changes in normal-appearing WM (NAWM) preceding conversion to WMH remains to be elucidated. This is especially important because there is increasing evidence that WMH progression accelerates

Received January 31, 2018; final revision received March 27, 2018; accepted April 5, 2018.

From the Department of Neurology, Donders Institute for Brain, Cognition, and Behaviour, Donders Center for Medical Neuroscience (E.M.C.v.L., M.I.B., I.W.M.v.U., A.M.T., F.-E.d.L.) and Department of Radiology and Nuclear Medicine, Diagnostic Image Analysis Group (M.G., B.P.), Radboud University Medical Center, Nijmegen, the Netherlands; Institute for Computing and Information Sciences (M.G.) and Donders Institute for Brain, Cognition, and Behaviour, Centre for Cognitive Neuroimaging (D.G.N.), Radboud University, Nijmegen, the Netherlands; Department of Neurology, Jeroen Bosch Ziekenhuis, 's-Hertogenbosch, the Netherlands (H.M.v.d.H.); and Erwin L. Hahn Institute for Magnetic Resonance Imaging, University of Duisburg-Essen, Germany (D.G.N.).

The online-only Data Supplement is available with this article at http://stroke.ahajournals.org/lookup/suppl/doi:10.1161/STROKEAHA.118.020980/-/DC1.

Correspondence to Frank-Erik de Leeuw, MD, PhD, Department of Neurology, Radboud University Medical Center, PO Box 9101, HP 935, 6500 HB Nijmegen, the Netherlands. E-mail frankerik.deleeuw@radboudumc.nl

over time.[12] Besides, progression was found most pronounced in participants with severe WMH,[12,13] suggesting differences in pathogenesis for mild versus severe WMH. More knowledge of the sequence of events that precedes the conversion of NAWM toward WMH might result in better identification of patients at risk for further WMH progression and the attendant clinical symptoms. This would especially be useful to identify in which individuals and at what moment preventive therapies could be beneficial.

In the present study, we, therefore, examined whether and when progression of WMH was preceded by changes in fluid-attenuated inversion recovery (FLAIR) and DTI values, using neuroimaging assessments at 3 time points for 9 years in 266 participants with SVD. We also studied differences between those with mild versus severe WMH. Finally, we analyzed the degree of WMH progression during follow-up according to baseline FLAIR and DTI measures.

Materials and Methods

Study Population

The RUN DMC study (Radboud University Nijmegen Diffusion Tensor and Magnetic Resonance Imaging Cohort) is a prospective cohort study of elderly with SVD that investigates risk factors and clinical consequences of SVD. The detailed study protocol has been published previously.[14] Of 503 baseline participants, 281 participants underwent repeated neuroimaging assessments at 3 time points (baseline in 2006, first follow-up in 2011, and second follow-up in 2015).[12] Fifteen participants were additionally excluded because of insufficient scan quality, yielding 266 participants for the present study. The Medical Review Ethics Committee region Arnhem-Nijmegen approved the study, and all participants gave written informed consent. The data that support the findings of this study are available from the corresponding author on request.

Vascular Risk Factors

We assessed the presence of hypertension, smoking, alcohol use, diabetes mellitus, and hypercholesterolemia at baseline by standardized questionnaires, as described previously.[14] We defined hypertension as use of antihypertensive agents and systolic blood pressure ≥140 mm Hg or diastolic blood pressure ≥90 mm Hg.[14]

Neuroimaging Protocol

MR images were acquired at 3 time points on 1.5-Tesla MRI (2006: MAGNETOM Sonata [Siemens]; 2011 and 2015: MAGNETOM Avanto [Siemens]) and included the following whole brain scans: T1-weighted 3-dimensional magnetization-prepared rapid gradient-echo (isotropic voxel size, 1.0 mm3), FLAIR (2006: voxel size, 0.5×0.5×5.0 mm; interslice gap, 1.0 mm; 2011 and 2015: voxel size, 0.5×0.5×2.5 mm; interslice gap, 0.5 mm), and DTI (2006: isotropic voxel size, 2.5 mm3; 4 unweighted scans, 30 diffusion-weighted scans at b=900 s/mm^2; 2011 and 2015: isotropic voxel size, 2.5 mm^3; 8 unweighted scans, 60 diffusion-weighted scans at b=900 s/mm^2). Full acquisition details have been described previously.[12,14]

Brain Tissue Segmentation and Volumetry

We calculated gray matter, WM, and cerebrospinal fluid volumes using SPM12 (http://www.fil.ion.ucl.ac.uk/spm/) unified segmentation routines on the T1 magnetization-prepared rapid gradient-echo images.[12] Next, we created binary WM masks from the WM segmentation maps. WMH were segmented semiautomatically using FLAIR and T1 sequences.[15] All segmentations were visually checked for artifacts and segmentation errors, blinded for clinical data. WMH volumes were calculated in milliliters, corrected for interscan differences in intracranial volume, and normalized to baseline intracranial volume.

DTI Processing

All diffusion-weighted images were denoised using a local principal component analyses filter[16] and corrected for cardiac, head motion, and eddy current artifacts simultaneously using the patching artefacts from cardiac and head motion (PATCH) algorithm,[17] as described previously.[18] Diffusion tensor and scalar parameters were calculated using DTIFit from FMRIB's Diffusion Toolbox (FDT), part of FMRIB Software Library (FSL).

Spatial Normalization

The spatial normalization process is described in the online-only Data Supplement, and a schematic overview of the spatial normalization process is displayed in Figure I in the online-only Data Supplement.

Normalization of FLAIR Values

To account for interindividual differences in FLAIR intensities, we normalized the FLAIR values.[11] We calculated the mean (μFLAIR) and SD (σFLAIR) of FLAIR values in the NAWM for each participant and defined a z score per voxel ($z\,\text{score} = \frac{\text{FLAIR} - \mu\text{FLAIR}}{\sigma\text{FLAIR}}$). The same procedure was applied to follow-up FLAIR images.

Definition of Regions

We created 4 masks for each participant: (1) remaining NAWM through all 3 MRI assessments, (2) NAWM converting into WMH in the second follow-up period (ie, between 2011 and 2015; in other words, converting into WMH after at least 5 years), (3) NAWM converting into WMH in the first follow-up period (ie, between 2006 and 2011; in other words, converting into WMH within 5 years), and (4) WMH at baseline (Figure 1). For mask A, we created a binary NAWM mask by subtracting the baseline and incident WMH masks from the baseline WM mask. Mask B was created by subtracting the mask with incident WMH voxels in the first time period from the mask with incident WMH voxels during the entire follow-up. Mask C was created by subtracting the baseline WMH map from the first follow-up WMH map. For mask D, we used the baseline WMH mask.

Statistical Analysis

We used t tests to compare mean baseline FLAIR, FA, and MD values in (1) remaining NAWM with values in (2) NAWM voxels converting into WMH in the second follow-up period, (3) NAWM converting into WMH in the first follow-up period, and (4) WMH. We additionally compared baseline FLAIR, MD, and FA values in NAWM converting into WMH and in WMH with values in remaining NAWM for all time points separately (ie, 2006–2011, 2011–2015, and overall 2006–2015) to validate the results. Further, we stratified by the modified Fazekas scale (mild, Fazekas 0–1; and severe, Fazekas 2–3)[19] to evaluate whether changes in microstructural integrity preceding WMH progression differed between participants with mild versus severe baseline WMH. We used 1-way ANOVA to investigate whether baseline FLAIR and DTI values in the previously mentioned 4 areas differed between participants with mild versus severe WMH. Additionally, we used repeated-measures ANOVA to investigate changes in MD values over time in the 4 areas. To investigate associations between baseline MD and FLAIR values and severity of WMH progression, we calculated quintiles of baseline MD and FLAIR values and analyzed WMH progression according to these strata, by 1-way ANOVA adjusted for age and sex, followed by a Bonferroni correction, and tested continuous linear trend per stratum. Statistical analyses were performed using Matlab, version 2014b, and SPSS Statistics, version 20.

Results

Baseline characteristics of the study population are presented in the Table. Mean age at baseline was 62.5 (SD,

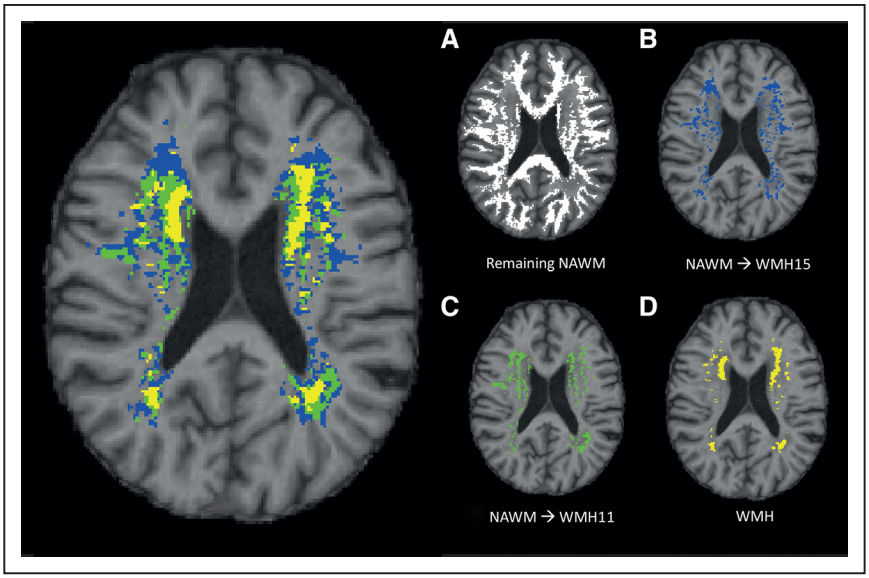

Figure 1. Progression of white matter hyperintensities (WMH) and definition of regions. **Left**, WMH progression during follow-up in a single representative patient: WMH at baseline (yellow), at first follow-up (green), and at second follow-up (blue). **Right**, Overview of the 4 masks included in analyses: (**A**) remaining normal-appearing white matter (NAWM), (**B**) NAWM converting into WMH in the second follow-up period, (**C**) NAWM converting into WMH in the first follow-up period, and (**D**) WMH.

7.8) years. Mean follow-up duration until first follow-up assessment was 5.4 (SD, 0.2) years and 8.7 (SD, 0.2) years until second follow-up assessment. Median WMH volume progressed from 2.2 mL (interquartile range, 0.8–6.1 mL) at baseline to 2.8 mL (interquartile range, 1.2–7.5 mL) at first follow-up and to 4.7 mL (interquartile range, 2.0–11.5

Table. Characteristics of the Study Population

	Study Population (n=266)	WMH Severity		Difference
		Fazekas 0–1 (n=211)	Fazekas 2–3 (n=55)	
Demographics				
Age, y	62.5±7.8	61.6±7.4	66.2±8.4	*P*<0.001
Male sex, n	157 (59.0)	129 (61.1)	28 (50.9)	*P*=0.218
MMSE score	28.6±1.3	28.7±1.3	28.3±1.5	*P*=0.037
Education, y	10.1±1.5	10.2±1.4	9.7±1.8	*P*=0.027
Vascular risk factors				
Hypertension, n	181 (68.0)	135 (64.0)	46 (83.6)	*P*=0.006
Diabetes mellitus, n	28 (10.5)	21 (10.0)	7 (12.7)	*P*=0.621
Hypercholesterolemia, n	112 (42.1)	89 (42.2)	23 (41.8)	*P*=1.000
Smoking, ever, n	191 (71.8)	148 (70.1)	43 (78.2)	*P*=0.313
Alcohol, glasses per wk	8.3±9.1	8.9±9.3	6.1±7.8	*P*=0.038
Body mass index, kg/m^2	27.1±4.1	27.2±4.2	26.5±3.8	*P*=0.220
Imaging characteristics				
Total brain volume, mL	1087.1±69.8	1095.8±65.4	1053.7±76.3	*P*<0.001
Gray matter volume, mL	621.2±48.6	627.1±46.4	598.6±50.7	*P*<0.001
White matter volume, mL	465.8±38.6	468.6±37.4	455.1±41.8	*P*=0.020
WMH volume, mL	2.2 (0.8–6.1)	1.4 (0.7–3.1)	14.8 (10.5–26.9)	*P*<0.001
Lacunes, n	52 (19.5)	25 (11.8)	27 (49.1)	*P*<0.001
Microbleeds, n	34 (12.8)	19 (9.0)	15 (27.3)	*P*=0.001
NAWM MD, 10^{-3} mm^2/s	0.85±0.04	0.84±0.03	0.88±0.04	*P*<0.001
NAWM FA	0.35±0.02	0.36±0.02	0.34±0.02	*P*<0.001

Data represent mean±SD, number of participants (%), or median (IQR). Comparisons between participants with Fazekas 0–1 and Fazekas 2–3 were performed by *t* test, χ^2, or Mann–Whitney *U* test. FA indicates fractional anisotropy; IQR, interquartile range; MD, mean diffusivity; MMSE, Mini-Mental State Examination; NAWM, normal-appearing white matter; and WMH, white matter hyperintensities.

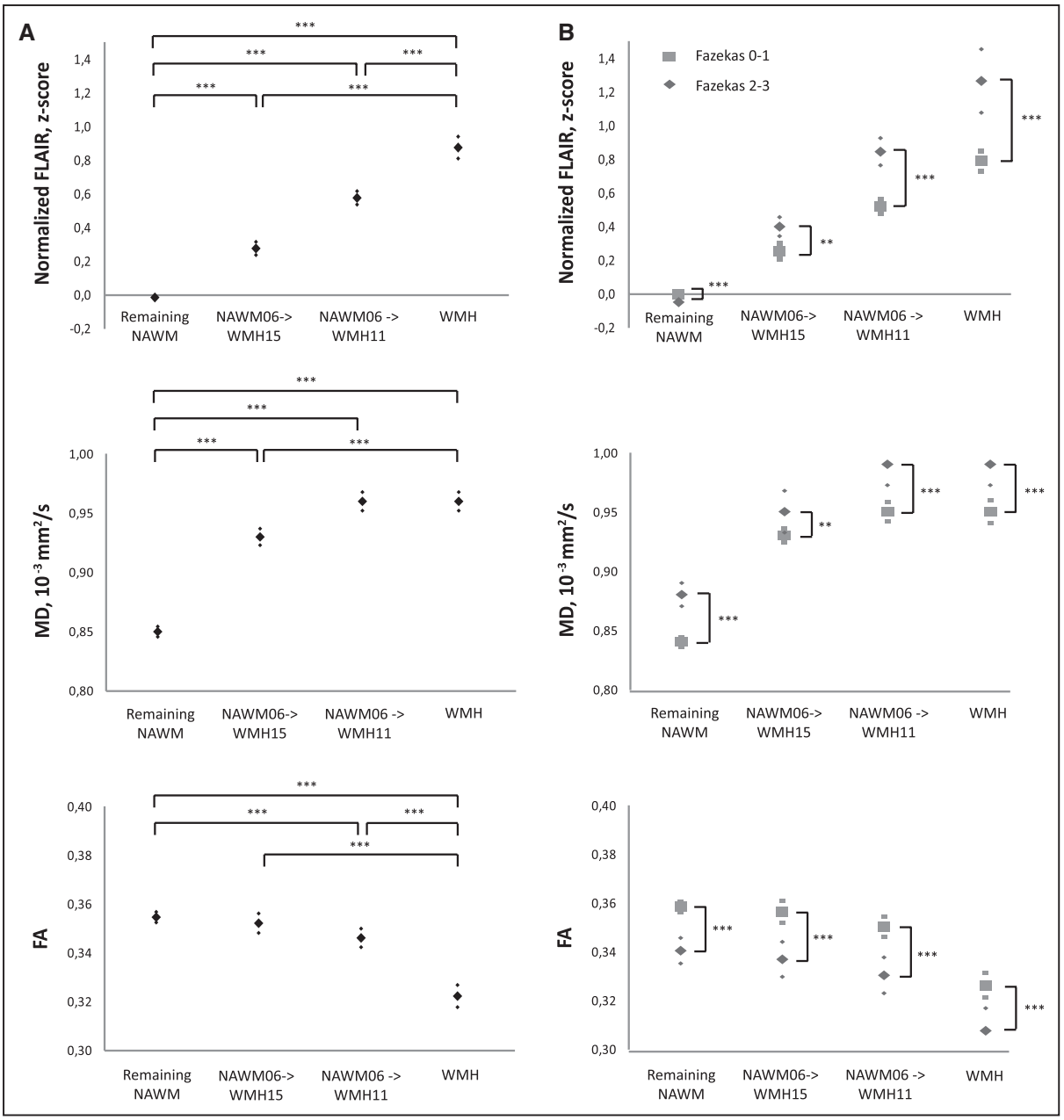

Figure 2. Baseline fluid-attenuated inversion recovery (FLAIR) and diffusion tensor imaging parameters in regions preceding white matter hyperintensities (WMH). Intensities of FLAIR, fractional anisotropy (FA), and mean diffusivity (MD) values at baseline in (1) remaining normal-appearing white matter (NAWM), (2) NAWM converting into WMH in the second follow-up period, (3) NAWM converting into WMH in the first follow-up period, and (4) WMH. **A**, Overall baseline FLAIR intensities and FA and MD values (mean with 95% confidence interval [CI]); statistical differences between the 4 areas are calculated by *t* tests. **B**, Baseline FLAIR intensities, FA, and MD values (mean with 95% CI) stratified by baseline Fazekas scores (Fazekas 0–1, light gray squares; Fazekas 2–3, dark gray diamonds); statistical differences between participants with Fazekas 0 to 1 and Fazekas 2 to 3 are calculated for the 4 areas separately, by 1-way ANOVA. ***P*<0.01, ****P*<0.001.

mL) at second follow-up. We observed lacunes in 52 participants (19.5%) at baseline and incident lacunes in 20.3% of participants. Presence of lacunes was more frequent in participants with severe WMH compared with participants with mild WMH (49.1% versus 11.8%; *P*<0.001). Participants who had not completed follow-up assessment were significantly older at baseline, had more vascular risk factors, and had more severe SVD characteristics (Table I in the online-only Data Supplement).

Baseline FLAIR and DTI Parameters in Areas Converting Into WMH

In Figure 2A, differences in baseline FLAIR, MD, and FA values are shown between the 4 areas. Compared with remaining NAWM areas through all 3 time points, NAWM areas converting into WMH in the second time interval had higher normalized FLAIR intensity and higher MD but similar FA values. NAWM areas converting into WMH in the first time interval had higher normalized FLAIR intensity, higher MD, and lower FA values

compared with remaining NAWM. In contrast, when compared with WMH, these NAWM areas converting into WMH in the first time period had lower normalized FLAIR intensity and higher FA, but MD values were similar between areas of WMH and areas converting into WMH in the first 5 years. Comparable differences in baseline FLAIR and DTI values were observed between the 4 areas when the follow-up periods were investigated separately (Table II in the online-only Data Supplement).

Baseline FLAIR and DTI Parameters by WMH Severity

Figure 2B illustrates baseline FLAIR and DTI measures in the 4 areas stratified by baseline WMH severity. Participants with Fazekas 2 to 3 had significantly higher normalized FLAIR and MD and lower FA values than those with Fazekas 0 to 1, in all WM areas, including the NAWM (P<0.005 for all comparisons). MD values in NAWM converting into WMH in the second time period in participants with Fazekas score 2 to 3 were similar to MD values in NAWM converting into WMH in the first time period and to WMH in participants with Fazekas 0 to 1.

Changes in MD Values Over Time

In Figure 3, changes in MD over time are shown for the 4 areas. The MD value in areas of remaining NAWM remained constant over time (Figure 3, diamonds). MD values in persisting WMH during the 9-year course continued to increase over time (circles in Figure 3; P<0.001 for all time periods). Interestingly, MD values in NAWM converting into WMH within the first 5 years were similar to MD values in persisting WMH at baseline and continued to increase over time (Figure 3, triangles; P<0.005 for all repeated-measures ANOVAs). MD values in NAWM converting into WMH between 5 and 10 years were slightly less elevated at baseline compared with WMH but continuously increased over time (P<0.005 for all time periods), reaching the level of MD in WMH areas at first follow-up in 2011 (Figure 3, squares).

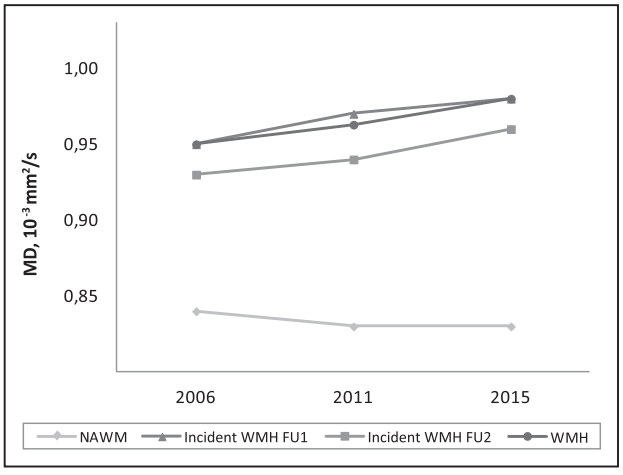

Figure 3. Changes in microstructural integrity over time in regions preceding white matter hyperintensities (WMH). Change in mean diffusivity (MD) values during the 3 time points in (1) remaining normal-appearing white matter (NAWM; diamonds), (2) NAWM converting into WMH in the second follow-up period (squares), (3) NAWM converting into WMH in the first follow-up period (triangles), and (4) WMH (circles).

WMH Progression According to Baseline FLAIR and DTI Parameters

We evaluated the progression of WMH at different levels of baseline FLAIR and DTI parameters by dividing the groups into quintiles. Cutoff values of quintiles were 0.816, 0.833, 0.848, and 0.874×10^{-3} mm^2/s for MD values and 315, 322, 329, and 336 for FLAIR values. The degree of WMH progression according to baseline MD and FLAIR strata in NAWM is presented in Figure 4. Higher baseline MD values in NAWM were associated with increased WMH progression during 9 years (mean difference, highest versus lowest quintile: 0.73 mL/y; 95% confidence interval, 0.26–1.19; P<0.001 adjusted for age and sex; overall P trend, <0.001). Higher FLAIR values at baseline were also associated with increased progression of WMH (mean difference, highest versus lowest quintile: 0.47 mL/y; 95% confidence interval, 0.03–0.91; P=0.025; overall P trend, <0.001).

Discussion

In this longitudinal study with 3 imaging assessments during 9 years, we observed that impaired microstructural integrity in the NAWM preceded conversion into WMH and that WM microstructural integrity declined over time. Participants with severe baseline WMH showed more loss of structural integrity compared with participants with mild WMH in all areas of the WM, including the remaining NAWM. These results suggest that WMH progression is an

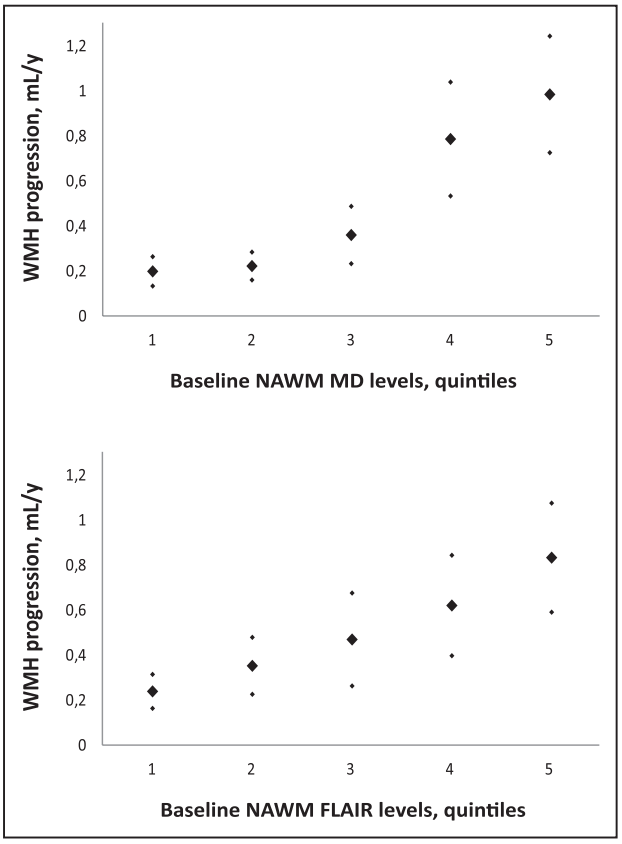

Figure 4. Progression of white matter hyperintensities (WMH), according to baseline mean diffusivity (MD) and fluid-attenuated inversion recovery (FLAIR) strata. WMH progression (in mL/y), stratified by baseline MD (**top**) and normalized FLAIR (**bottom**) quintiles. NAWM indicates normal-appearing white matter.

ongoing process characterized by loss of WM microstructural integrity occurring years before WMH can be detected on conventional MRI.

These results are in line with 2 longitudinal studies showing changes in baseline DTI and FLAIR signal intensities that were related to incident WMH at follow-up, with mean follow-up duration of 3.5 and 3.7 years.[10,11] Here, we extended these findings by adding an additional time point with a total follow-up of 9 years, which enabled us to distinguish between NAWM converting into WMH within the first and the second time period. We observed that baseline MD values were higher in NAWM areas converting into WMH within 5 years than in NAWM areas that converted into WMH between 5 and 9 years. Besides, MD values continued to increase over time. The continuously ongoing decline of microstructural integrity within the WM underlines that WMH progression visible on conventional FLAIR imaging is only the tip of the iceberg with underlying loss of microstructural integrity that can only be visualized using more advanced neuroimaging techniques.

Participants with severe baseline WMH showed higher normalized FLAIR and MD values and lower FA values than participants with mild baseline WMH in all areas, including the remaining NAWM. Differences between participants with mild versus severe baseline WMH have been reported before with respect to progression of their WMH, suggesting heterogeneity in pathogenesis of mild versus severe WMH.[12,13,20] Our observed differences in microstructural integrity between participants with mild and severe baseline WMH in both remaining NAWM and WMH confirm and extend this hypothesis. The observation of impaired microstructural integrity in remaining NAWM in participants with baseline Fazekas 2 to 3 indicates that NAWM is not as normal as one would expect from conventional MRI and underlines the hypothesis of a continuous, ongoing disease of the WM in SVD. Moreover, it might be an explanation for the observation that WMH progression was most pronounced in participants with severe WMH at baseline.[12]

The findings that the microstructural integrity within WMH was more impaired in participants with severe baseline WMH than in participants with mild baseline WMH and also continuously declined over time within WMH in both groups suggest that not only NAWM but also WMH is heterogeneous. This heterogeneity of microstructural integrity in WMH might explain clinical variances observed in subjects with similar SVD severity. For example, participants with impaired WMH microstructural integrity might have more severe clinical symptoms compared with participants with the same degree of WMH but with higher microstructural integrity in their WMH. This hypothesis is supported by findings in patients with SVD, showing that patients with severe loss of microstructural integrity within their WMH showed decreased cognitive performance and had higher risk of Parkinsonian signs, independent of WMH volume.[21,22]

Our findings can be clinically relevant because differences in microstructural integrity between remaining NAWM and incident WMH suggest that it would be possible to predict which NAWM voxels will convert into WMH, based on baseline FLAIR and DTI values. Our observation that impaired microstructural integrity at baseline was associated with more extensive WMH progression during 9 years implies that measures of microstructural integrity can possibly be used as biomarker for WMH progression, as well as for personalized treatment approaches. Increasing evidence suggests that endothelial dysfunction might be an important factor in the pathogenesis of SVD because loss of WM microstructure has been associated with reduced endothelial function.[23] Although speculative, potential treatment strategies might target the brains' microvascular endothelium with endothelin antagonists or NO donors,[24] although randomized controlled trials are required. For now, we would argue a stringent control of vascular risk factors according to current guidelines, until further data from randomized controlled trials are available.

Major strengths of this study include the longitudinal design of our study with 3 neuroimaging assessments during 9 years, which enabled us to elaborate on the temporal dynamics of WMH progression. Furthermore, the availability of these 3 time points enabled us to validate the findings in the other follow-up periods.

Several methodological issues and limitations deserve consideration. First, differences in MRI scanner and FLAIR sequences between baseline and first follow-up might be a potential source of bias because this might have led to differences in coregistrations of the FLAIR images and WMH masks to Montreal Neurological Institute space between baseline and first and second follow-up images. However, we consider this unlikely because we performed several analyses to estimate and minimize the effects of possible interscan effects. Coregistrations of all images to Montreal Neurological Institute space have been performed with great caution using an intermediate subject template and the most robust and accurate registration routines.[25] Besides, in additional analyses, we only used those WMH voxels that were classified as WMH both at baseline and at follow-up imaging, reducing the risk of bias because of possible overestimation of WMH at baseline. These analyses revealed similar results (data not shown). Moreover, we validated our findings by repeating analyses for all time periods separately (Table II in the online-only Data Supplement). The results for the first follow-up and the overall time interval were comparable with the results for the second follow-up period in which scanner and sequence protocols remained identical. Hence, it is unlikely that change in scanner between baseline and first follow-up biased the results. Second, so-called partial volume effects might have introduced a potential bias, that is, NAWM voxels around the border of existing WMH can contain a fraction of WMH signal intensity that affects measurements in that voxel. It is possible that this has led to an overestimation of intensities in the masks consisting of NAWM voxels that converted into WMH during follow-up when WMH progression occurred adjacent to already existing WMH. However, it cannot explain all differences, especially also because NAWM voxels remote from preexisting WMH were included in the masks. Third, because of the long-term follow-up of our study, a proportion of the participants was unable to complete the entire follow-up. This attrition bias might have led to an underestimation of the effects because those lost to follow-up had more severe SVD already at baseline (Table I in the online-only Data Supplement), and

severity of WMH at baseline is associated with progression of WMH.[12,13,20] A fourth limitation might be that we would need even more advanced neuroimaging protocols to visualize the underlying mechanisms of final conversion of NAWM into WMH because MD values in NAWM that converted into WMH within 5 years were similar to MD values in WMH. Otherwise, it might be that other processes, such as secondary neurodegeneration, hypoperfusion, inflammation, or small acute infarctions, play a role in the final conversion into WMH. Studies with more follow-up ascertainments on shorter time intervals may shed more light on the underlying processes of the final conversion into WMH. Because there is increasing awareness that SVD exerts its clinical effects by affecting remote brain structures,[26–29] future studies should also address the role of gray matter atrophy and how it is affected by WMH progression. In addition, it would be of interest to study changes in microstructural integrity preceding incident lacunes because the presence of lacunes plays an important role in the development of cognitive deficits as well.[30,31]

In conclusion, WMH progression visible on conventional FLAIR imaging is only the tip of the iceberg with underlying loss of WM microstructural integrity that continuously declines over time. These findings indicate that microstructural measures derived from DTI can predict the development of WMH years before they are visible on conventional neuroimaging. Future studies should elaborate on the possibility to use these measures of microstructural integrity for personalized treatment approaches.

Disclosures

Dr Tuladhar is supported by a junior staff member grant of the Dutch Heart Foundation (grant No. 2016 T044). Dr de Leeuw is supported by a clinical established investigator grant of the Dutch Heart Foundation (grant No. 2014 T060) and by a VIDI innovational grant from the Netherlands Organisation for Health Research and Development (ZonMw grant 016.126.351).

References

1. Wardlaw JM, Smith EE, Biessels GJ, Cordonnier C, Fazekas F, Frayne R, et al; Standards for Reporting Vascular Changes on Neuroimaging (STRIVE v1). Neuroimaging standards for research into small vessel disease and its contribution to ageing and neurodegeneration. *Lancet Neurol*. 2013;12:822–838. doi: 10.1016/S1474-4422(13)70124-8.
2. de Leeuw FE, de Groot JC, Achten E, Oudkerk M, Ramos LM, Heijboer R, et al. Prevalence of cerebral white matter lesions in elderly people: a population based magnetic resonance imaging study. The Rotterdam Scan study. *J Neurol Neurosurg Psychiatry*. 2001;70:9–14.
3. van Dijk EJ, Prins ND, Vermeer SE, Koudstaal PJ, Breteler MM. Frequency of white matter lesions and silent lacunar infarcts. *J Neural Transm Suppl*. 2002:25–39.
4. Prins ND, Scheltens P. White matter hyperintensities, cognitive impairment and dementia: an update. *Nat Rev Neurol*. 2015;11:157–165. doi: 10.1038/nrneurol.2015.10.
5. Debette S, Markus HS. The clinical importance of white matter hyperintensities on brain magnetic resonance imaging: systematic review and meta-analysis. *BMJ*. 2010;341:c3666.
6. Vernooij MW, de Groot M, van der Lugt A, Ikram MA, Krestin GP, Hofman A, et al. White matter atrophy and lesion formation explain the loss of structural integrity of white matter in aging. *Neuroimage*. 2008;43:470–477. doi: 10.1016/j.neuroimage.2008.07.052.
7. Wardlaw JM, Valdés Hernández MC, Muñoz-Maniega S. What are white matter hyperintensities made of? Relevance to vascular cognitive impairment. *J Am Heart Assoc*. 2015;4:001140. doi: 10.1161/JAHA.114.001140.
8. Soares JM, Marques P, Alves V, Sousa N. A hitchhiker's guide to diffusion tensor imaging. *Front Neurosci*. 2013;7:31. doi: 10.3389/fnins.2013.00031.
9. Jones DK, Lythgoe D, Horsfield MA, Simmons A, Williams SC, Markus HS. Characterization of white matter damage in ischemic leukoaraiosis with diffusion tensor MRI. *Stroke*. 1999;30:393–397.
10. de Groot M, Verhaaren BF, de Boer R, Klein S, Hofman A, van der Lugt A, et al. Changes in normal-appearing white matter precede development of white matter lesions. *Stroke*. 2013;44:1037–1042. doi: 10.1161/STROKEAHA.112.680223.
11. Maillard P, Carmichael O, Harvey D, Fletcher E, Reed B, Mungas D, et al. FLAIR and diffusion MRI signals are independent predictors of white matter hyperintensities. *AJNR Am J Neuroradiol*. 2013;34:54–61. doi: 10.3174/ajnr.A3146.
12. van Leijsen EMC, van Uden IWM, Ghafoorian M, Bergkamp MI, Lohner V, Kooijmans ECM, et al. Nonlinear temporal dynamics of cerebral small vessel disease: the RUN DMC study. *Neurology*. 2017;89:1569–1577. doi: 10.1212/WNL.0000000000004490.
13. Schmidt R, Enzinger C, Ropele S, Schmidt H, Fazekas F; Austrian Stroke Prevention Study. Progression of cerebral white matter lesions: 6-year results of the Austrian Stroke Prevention Study. *Lancet*. 2003;361:2046–2048.
14. van Norden AG, de Laat KF, Gons RA, van Uden IW, van Dijk EJ, van Oudheusden LJ, et al. Causes and consequences of cerebral small vessel disease. The RUN DMC study: a prospective cohort study. Study rationale and protocol. *BMC Neurol*. 2011;11:29. doi: 10.1186/1471-2377-11-29.
15. Ghafoorian M, Karssemeijer N, van Uden IW, de Leeuw FE, Heskes T, Marchiori E, et al. Automated detection of white matter hyperintensities of all sizes in cerebral small vessel disease. *Med Phys*. 2016;43:6246. doi: 10.1118/1.4966029.
16. Manjón JV, Coupé P, Concha L, Buades A, Collins DL, Robles M. Diffusion weighted image denoising using overcomplete local PCA. *PLoS One*. 2013;8:e73021. doi: 10.1371/journal.pone.0073021.
17. Zwiers MP. Patching cardiac and head motion artefacts in diffusion-weighted images. *Neuroimage*. 2010;53:565–575. doi: 10.1016/j.neuroimage.2010.06.014.
18. van Uden IW, Tuladhar AM, van der Holst HM, van Leijsen EM, van Norden AG, de Laat KF, et al. Diffusion tensor imaging of the hippocampus predicts the risk of dementia: the RUN DMC study. *Hum Brain Mapp*. 2016;37:327–337. doi: 10.1002/hbm.23029.
19. Fazekas F, Chawluk JB, Alavi A, Hurtig HI, Zimmerman RA. MR signal abnormalities at 1.5 T in Alzheimer's dementia and normal aging. *AJR Am J Roentgenol*. 1987;149:351–356. doi: 10.2214/ajr.149.2.351.
20. van Dijk EJ, Prins ND, Vrooman HA, Hofman A, Koudstaal PJ, Breteler MM. Progression of cerebral small vessel disease in relation to risk factors and cognitive consequences: Rotterdam Scan study. *Stroke*. 2008;39:2712–2719. doi: 10.1161/STROKEAHA.107.513176.
21. de Laat KF, van Norden AG, van Oudheusden LJ, van Uden IW, Norris DG, Zwiers MP, et al. Diffusion tensor imaging and mild parkinsonian signs in cerebral small vessel disease. *Neurobiol Aging*. 2012;33:2106–2112. doi: 10.1016/j.neurobiolaging.2011.09.001.
22. van Norden AG, de Laat KF, van Dijk EJ, van Uden IW, van Oudheusden LJ, Gons RA, et al. Diffusion tensor imaging and cognition in cerebral small vessel disease: the RUN DMC study. *Biochim Biophys Acta*. 2012;1822:401–407. doi: 10.1016/j.bbadis.2011.04.008.
23. Johnson NF, Gold BT, Brown CA, Anggelis EF, Bailey AL, Clasey JL, et al. Endothelial function is associated with white matter microstructure and executive function in older adults. *Front Aging Neurosci*. 2017;9:255. doi: 10.3389/fnagi.2017.00255.
24. Bath PM, Wardlaw JM. Pharmacological treatment and prevention of cerebral small vessel disease: a review of potential interventions. *Int J Stroke*. 2015;10:469–478. doi: 10.1111/ijs.12466.
25. Klein A, Andersson J, Ardekani BA, Ashburner J, Avants B, Chiang MC, et al. Evaluation of 14 nonlinear deformation algorithms applied to human brain MRI registration. *Neuroimage*. 2009;46:786–802. doi: 10.1016/j.neuroimage.2008.12.037.
26. Duering M, Righart R, Csanadi E, Jouvent E, Hervé D, Chabriat H, et al. Incident subcortical infarcts induce focal thinning in connected cortical regions. *Neurology*. 2012;79:2025–2028. doi: 10.1212/WNL.0b013e3182749f39.
27. Lambert C, Benjamin P, Zeestraten E, Lawrence AJ, Barrick TR, Markus HS. Longitudinal patterns of leukoaraiosis and brain atrophy in symptomatic small vessel disease. *Brain*. 2016;139(pt 4):1136–1151. doi: 10.1093/brain/aww009.

28. Grau-Olivares M, Arboix A, Junqué C, Arenaza-Urquijo EM, Rovira M, Bartrés-Faz D. Progressive gray matter atrophy in lacunar patients with vascular mild cognitive impairment. *Cerebrovasc Dis*. 2010;30:157–166. doi: 10.1159/000316059.
29. Smith EE, Arboix A. Focal cortical thinning is caused by remote subcortical infarcts: spooky action at a distance. *Neurology*. 2012;79:2016–2017. doi: 10.1212/WNL.0b013e3182749f6e.
30. Vermeer SE, Prins ND, den Heijer T, Hofman A, Koudstaal PJ, Breteler MM. Silent brain infarcts and the risk of dementia and cognitive decline. *N Engl J Med*. 2003;348:1215–1222. doi: 10.1056/NEJMoa022066.
31. Blanco-Rojas L, Arboix A, Canovas D, Grau-Olivares M, Oliva Morera JC, Parra O. Cognitive profile in patients with a first-ever lacunar infarct with and without silent lacunes: a comparative study. *BMC Neurol*. 2013;13:203. doi: 10.1186/1471-2377-13-203.